Journal of Cleaner Production 334 (2022) 130080

Contents lists available at ScienceDirect

Journal of Cleaner Production

journal homepage: www.elsevier.com/locate/jclepro

Effects of the lignite bioorganic fertilizer on greenhouse gas emissions and pathways of nitrogen and carbon cycling in saline-sodic farmlands at Northwest China

Zhijun Chen [a,c], Guanhua Huang [a,b,*], Yue Li [a,b], Xuechen Zhang [a,b], Yunwu Xiong [a,b], Quanzhong Huang [a,b], Song Jin [d,e]

[a] Center for Agricultural Water Research, China Agricultural University, Beijing, 100083, PR China
[b] Chinese-Israeli International Center for Research and Training in Agriculture, China Agricultural University, Beijing, 100083, PR China
[c] College of Water Conservancy, Shenyang Agricultural University, Shenyang, 110866, PR China
[d] Advanced Environmental Technologies LLC, Fort Collins, CO, 80525, USA
[e] Department of Civil and Architectural Engineering, University of Wyoming, Laramie, WY, 82071, USA

ARTICLE INFO

Handling Editor: Bin Chen

Keywords:
Nitrogen fixation process
Nitrification process
Net primary production
Methanogenesis

ABSTRACT

Mitigating climate change and improving food production are major challenges worldwide. Applications of lignite-based bioorganic products (or lignite-based fertilizer) can improve soil physicochemical properties and crop production in saline-sodic farmland. However, little is known about the effects of lignite bioorganic fertilizer (LBF) on greenhouse gas (GHG) emissions and climate change mitigation. Thus, a two-year field experiment was conducted in saline-sodic farmlands in the upper Yellow River basin, Northwest China. The field experiment comprised six treatments, including a negative control without any organic fertilizer (CK), a positive control amended with sheep manure (FYM), and four treatments amended with 1.5 (LBF1), 3 (LBF2), 4.5 (LBF3), and 7.5 t ha^{-1} (LBF4) LBF. The results showed that the LBF treatments decreased the emissions of CH_4 and CO_2 while increasing N_2O emissions when the application rate was over 3 t ha^{-1}. Additionally, FYM treatment acted as a CH_4 source, while LBF2 and LBF3 treatments were both CH_4 sinks. The LBF3 treatment had the highest net ecosystem carbon budget (NECB) and the lowest net ecosystem global warming potential (NGWP), which were 6.04 and 4.82 t ha^{-1} and -22.09 and −17.39 t ha^{-1} higher than those of the CK treatment in 2019 and 2020, respectively. Moreover, the net ecosystem economic budget (NEEB) of the LBF2 and LBF3 treatments was higher than that of the other treatments. Compared with the CK treatment, the FYM treatment increased the NCEB and decreased NGWP but it also decreased the NEEB. For nitrogen and carbon cycling, the LBF3 treatment increased almost all gene families involved in nitrogen cycling, except for *nirA* and *hao*, while the FYM treatment reduced the *nirKS, norBC*, *nosZ*, and *hao* gene families. The modules for carbohydrate metabolism and methanogenesis were also reduced by the LBF treatments. In conclusion, the LBF2 and LBF3 treatments had higher NECB, NGWP, and NEEB, indicating that the application of lignite bioorganic fertilizer at 3.0–4.5 t ha^{-1} is appropriate for climate change mitigation in saline-sodic farmlands in the upper Yellow River basin, Northwest China.

1. Introduction

With global warming and population growth, mitigating climate change and improving food production are significant challenges worldwide (Zhang et al., 2018; Shakoor et al., 2021a). Global warming will be irreversible in the future, and the average global temperature will increase by approximately 1.5 °C in the next 20 years (IPCC, 2021). However, reducing greenhouse gas (GHG) emissions is an effective method to keep the atmosphere from becoming warmer in the future. Although the primary source for GHG is the massive burning of fossil fuels and rapid deforestation, human-caused GHG from agricultural soil contributes almost 10–14% of the total GHG through manure and synthetic fertilizer (Paustian et al., 2016; Shakoor et al., 2020). Soil salinization has become one of the critical constraints for the sustainable

; GHG, greenhouse gas; NECB, net ecosystem carbon budget; NGWP, net ecosystem global warming potential; NEEB, net ecosystem economic budget.

* Corresponding author. Center for Agricultural Water Research, China Agricultural University, Beijing, 100083, PR China.
E-mail address: ghuang@cau.edu.cn (G. Huang).

https://doi.org/10.1016/j.jclepro.2021.130080
Received 11 October 2021; Received in revised form 23 November 2021; Accepted 11 December 2021
Available online 14 December 2021
0959-6526/

development of global agriculture. Around the world, the total areas of saline and sodic soil are approximately 397 and 434 million hectares, respectively (Daliakopoulos et al., 2016; Ghosh et al., 2017). In China, the Hetao Irrigation District (HID), located in the upper Yellow River basin, is one of the main grain production areas; however, crop growth in HID is limited by soil salinization caused by the shallow groundwater table, scarce precipitation, and large evaporation. Soil salinization has also been proven to be the major factor for reconstructing the global distribution of soil microorganisms and suppressing nitrogen and carbon cycling pathways (Lozupone and Knight, 2007; Kelly et al., 2021; Yang et al., 2021). Thus, the GHG emissions in saline-sodic farmland are significantly limited (Tang et al., 2016). For instance, Zhang et al. (2017) reported that higher soil pH and salinity reduced the emissions of CO_2, CH_4, and N_2O, subsequently lowering the global warming potential. These results led to the hypothesis that improving crop growth could change saline-sodic farmland from GHG sources to GHG sinks by increasing photosynthesis and crop production. Above all, ameliorative methods need to be taken to improve the soil quality of saline-sodic soil to increase crop production and mitigate climate change.

In recent years, organic matter, e.g., farmyard manure (FYM) and raw lignite, has been used to improve soil quality and productivity (Mahmood et al., 2017; Amoah-Antwi et al., 2020). It has been widely recognized that applying FYM, a readily available organic fertilizer, can increase soil organic matter and improve crop yield (Loper et al., 2010; Zhang et al., 2015; Zhen et al., 2014). For instance, Mahmood et al. (2017) reported that the application of FYM (15 t ha^{-1}) increased soil organic carbon by 85%–90%, decreased pH and bulk density by 4%–7% and 10%, respectively, and improved maize yield by 52%–77%. Previous studies have consistently proven that the addition of FYM also improved GHG emissions from the soil and global warming potential due to an increase in soil respiration (Zhou et al., 2017; Shakoor et al., 2021b). However, those studies only evaluated the impacts of FYM on GHGs emitted from the soil, and the increased carbon sink from the atmosphere achieved by improvement of photosynthesis was barely reported. Therefore, the effects of the application of FYM on the net carbon budget and net GHG emission from the crop system were largely unclear, especially in saline-sodic farmland. Moreover, the application of FYM provided more organic carbon to the soil, which could improve nitrogen and carbon cycling in crop systems. However, to the best of our knowledge, there is still a lack comprehensive analyses of the influence of FYM on nitrogen and carbon cycling.

Lignite has received attention from researchers as a potential soil conditioner in recent years (Little et al., 2014; Tsetsegmaa et al., 2018). Studies have demonstrated that applying lignite or lignite-based fertilizer can improve soil organic matter, in turn increasing nutrient holding and water retention ability as well as crop yield (Nan et al., 2015; Dubey et al., 2019). For instance, Akimbekov et al. (2020) reported that compared with a control treatment, applying humic acid derived from lignite improved potato growth and tuber yield by 54.9% and 66.4%, respectively. Although the application of lignite or lignite-based fertilizer has been demonstrated to modify soil physicochemical properties and in turn improve crop production, the effects of lignite or lignite products on GHG emissions and net ecosystem carbon budgets (NECBs) are not well understood. Additionally, lignite or lignite bioorganic fertilizer contains a variety of organic compounds (Akimbekov et al., 2020; Li et al., 2020), which could provide many substrates for nitrogen and carbon metabolism and then impact the nitrogen and carbon cycling pathways.

Above all, although previous studies have proven that the application of farmyard manure and lignite or lignite-based fertilizer could improve soil quality, the impacts of farmyard manure and lignite-based fertilizer on GHG emissions, the carbon budget, net global warming potential, and nitrogen and carbon cycling pathways are largely unclear. Thus, the main objectives of our research are (1) to assess the effects of farmyard manure and lignite-based fertilizer on soil GHG emissions; (2) to study the impacts of farmyard manure and lignite-based fertilizer on net ecosystem carbon and the economic budget; and (3) to explore the influence of farmyard manure and lignite-based fertilizer on nitrogen and carbon cycling pathways in saline-sodic farmlands in the upper Yellow River basin, Northwest China.

2. Materials and methods

2.1. Experimental site and experimental design

The field experiments were conducted in 2019 and 2020 at the Hetao Experimental Station of China Agricultural University (41°09′N, 107°39′E, 1042 m.a.s.l) in the upper Yellow River basin, Northwest China. The experimental site is characterized by a semiarid temperate continental climate with 2200–2400 mm of potential evaporation. The annual mean temperature and precipitation are 6.8 °C and 160–180 mm, respectively. Approximately 50% of the annual precipitation occurs from July to September. In the study area, the average sunshine duration is approximately 3230 h, and frost-free conditions last for approximately 130 d, with a maximum frozen soil depth of 1.2 m (Li et al., 2020). The details of rainfall and air temperature during sunflower growth period were illustrated in Fig.1.

In the field experiment, six treatments were applied: the control treatment without organic fertilizer (CK), the farmyard manure treatment amended with sheep manure at 21 t ha^{-1} (FYM), and four treatments amended with lignite bioorganic fertilizer at 1.5 (LBF1), 3 (LBF2), 4.5 (LBF3) and 7.5 t ha^{-1} (LBF4). An application rate of 21 t ha^{-1} was recommended by local farmers, and the rate of lignite bioorganic fertilizer application was chosen based on the manufacturers' recommended value of 3 t ha^{-1}. The basic properties of the lignite bioorganic fertilizer are listed in Table 1. All plots were arranged following a completely randomized block method in this study, and each plot had an area of 126 m^2 (7 m × 18 m). Basic physicochemical properties are summarized in Table 1. As shown in Table 1, the pH, exchangeable sodium saturation percentage (ESP), saturated electrical conductivity (EC_e), saturated sodium adsorption ratio (SAR_e), and soil bulk density are 9.4, 56 (mmoles l^{-1})$^{0.5}$, 9.3 ds m^{-1}, 16.3%, and 1.62, respectively in 0–20 cm, indicating that soils of the study area saline-sodic and of poor physical and chemical properties.

The lignite bioorganic fertilizer (LBF) is a novel, biochemically processed lignite product. It has been certified by the OMRI and EU as an organic fertilizer and soil conditioner (provided by Apaxfon Bioscience and Technologies Ltd., CO, "Apaxfon", Baotou, Inner Mongolia, China). Lignite bioorganic fertilizer (LBF) is produced with lignite through a series of physicochemical and biochemical reactions. LBF contains a variety of organic compounds, ranging from large humic matter to small soluble organic acids. The basic properties of the LBF and FYM are listed in Table 1.

Sunflower (Guaner No. 1) was sown on June 2nd and June 5th and harvested on September 16th and September 18th in 2019 and 2020, respectively. Alternating wide and narrow rows with a wide-row spacing of 100 cm and narrow-row spacing of 40 cm was adopted in this study. Thus, the average row spacing was 70 cm. Additionally, the plant spacing was approximately 50 cm, resulting in a plant density of approximately 28,500 plants ha^{-1}. The narrow rows were covered by black plastic film with a width of 70 cm and a thickness of 0.008 mm. FYM and LBF were supplied as base fertilizers before seeding. In terms of chemical fertilizer, 81.0 kg ha^{-1} N, 90.3 kg ha^{-1} P, and 30 kg ha^{-1} K were applied as base fertilizers, and at the budding stage of sunflowers, 25.2 kg ha^{-1} N, 9.2 kg ha^{-1} P, and 5.0 kg ha^{-1} K were applied. To reduce the limitations of salinity and sodicity on crop emergence, 1800 m^3 ha^{-1} water from the Yellow River was applied to the field before seeding. No irrigation was applied during the growing period of sunflower.

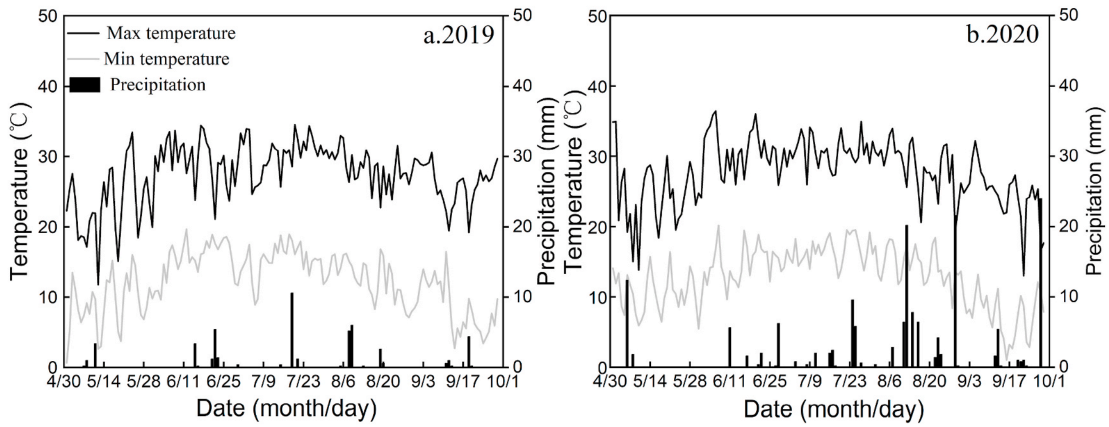

Fig. 1. Daily minimum and maximum temperatures, and precipitation at the experimental site throughout the sunflower growing seasons (2019 and 2020).

Table 1
The physicochemical properties of the soil, lignite bioorganic fertilizer and farmyard manure.

Property	Soil	Lignite bioorganic fertilizer	Farmyard manure
Sand (%)	40.5	–	–
Silt (%)	53.5	–	–
Clay (%)	6.03	–	–
Texture	Silt loam	–	–
Bulk density (g cm^{-3})	1.62	–	0.7
pH	9.4	8.48	8.0
ECe (ds m^{-1})	9.3	30.8	–
SARe (mmoles $l^{-1})^{0.5}$	56	–	–
ESP (%)	16.3	–	–
SOM (g kg^{-1})	6.9	836	530
Total N (%)	0.06	3.09	2.22
Total C (%)	1.61	36.63	24.67
C/N ratio	26.8	11.86	11.1
AN (mg kg^{-1})	12.5	280.4	–
P (P_2O_5, mg kg^{-1})	10.6	42,100	–
K (K_2O, mg kg^{-1})	258.5	27,800	–
AN + P_2O_5+ K_2O (%)	–	7.0	6.3

Note: EC_e represents the electrical conductivity of saturated paste extract; SAR_e represents the sodium adsorption ratio of saturated paste extract; ESP represents the exchangeable sodium saturation percentage; SOM represents the soil organic matter; AN represents the available nitrogen; AP represents the available phosphorous; AK represents the available potassium.

2.2. Sampling and measurements

2.2.1. Measurement of greenhouse gas fluxes

Soil gases were collected using a static chamber method approximately every ten days during the sunflower growth period each year (Li et al., 2020). The static chambers were placed between two rows of sunflower plants. Five gas samples for each plot were collected at 9:00 to 11:00 with 10-min intervals. The concentrations of three main greenhouse gases, CO_2, CH_4, and N_2O, were then measured by GC-2014 gas chromatography (Shimadzu Scientific Instruments) within 48 h. The static chamber was made of stainless steel with a size of 40 cm × 40 cm × 40 cm. The detailed processes for measuring GHG can be found in Li et al. (2020) and Wang et al. (2014). The flux and total CO_2, CH_4, and N_2O emissions were calculated using Eqs. (1) and (2), respectively.

$$F = \frac{dc}{dt} \cdot \frac{M}{V_0} \cdot \frac{P}{P_0} \cdot \frac{273}{(273+t)} \cdot H \tag{1}$$

$$E = 24 \times \left[\sum_{i=1}^{n-1} \frac{(F_i + F_{i+1})}{2} \Delta d\right] \times 10^{-2} \tag{2}$$

where F is the greenhouse gas emission flux, mg m^{-2} h^{-1}; d_c/d_t is the variation ratio of the measured greenhouse gas, mg m^{-3} h^{-1}; M is the molar mass of greenhouse gas molecules, g mol^{-1}; t is the air temperature, °C; P and P_0 are actual and atmospheric pressure, KPa, respectively; H is the height of the chamber, m; E is the total emissions of greenhouse gas during the sunflower growth period, kg ha^{-1}; F_{i+1} and F_i are the greenhouse gas fluxes measured at times i+1 and i, respectively, mg m^{-3} h^{-1}; and $\triangle d$ is the number of days between F_{i+1} and F_i.

2.2.2. Soil properties and plant samples

In this study, soil samples in the 0–10 cm soil layer were taken to measure NH_4^+-N, NO_3^--N, pH, electrical conductivity (EC), and soil water content immediately after gas collection. NH_4^+-N and NO_3^--N were examined by ultraviolet spectrophotometry (UV-3100, China), and the details of the measurement processes were similar to those of Li et al. (2020). The EC and pH were potentiometrically measured using a soil/solution ratio of 1:5 (Li et al., 2021). The soil water content was determined by the thermogravimetric method. The soil temperature was measured using a geothermometer (WNY-12, China) inserted to a depth of 10 cm near the static chamber.

Before experiment, soil samples collected from 0 to 20 cm top layer, lignite bioorganic fertilizer, and farmyard manure were taken to measure their basic properties, including soil particle-size distribution, bulk density, pH, saturate electronic conductivity (EC_e), soil cation exchange capacity (CEC), sodium adsorption ratio (SAR_e), exchangeable sodium (ES), exchangeable sodium percentage (ESP), total N and C, available N (AN), P (AP), and K (AK), and soil organic matter (SOM). Soil particle-size distributions were determined using the laser diffraction particle size analyze (Mastersizer 2000, the UK) (Li et al., 2020), and soil texture was determined using the US textural classification triangle (Li et al., 2020). Soil bulk density was measured using the gravimetric method. CEC was measured by the sodium acetate method (Chapman, 1965). ES was determined by the ammonium acetate method (Bao, 2000). ESP was determined as the ratio of ES to CEC. SAR_e was the ratio of soluble Na^+ to $(0.5Ca^{2+}+0.5Mg^{2+})$ ˆ0.5 (Zaman et al., 2018). The soluble Na^+, Ca^{2+}, and Mg^{2+} were determined using a potentiometric titration (Titrator Excellence T5, Switzerland) (Bao, 2000). Total N and C were determined using an element analyzer (Vario Macro CN, Germany). AN was the sum of NH_4^+-N and NO_3^--N, which was determined by ultraviolet spectrophotometer (UV-3100, China). AK was determined using the ammonium acetate extraction-flame photometry (Model 410 Flame Photometer, US). AP was determined by the sodium bicarbonate extraction-Mo-Sb colorimetry method (Li et al., 2021). SOM was determined using the potassium dichromate volumetric-external heating method (Li et al., 2021).

In this study, sunflowers from a 10 m^2 area in each plot were harvested during the late-maturing stage to measure yield. In addition, three plants in each plot were selected for measuring aboveground dry biomass. To avoid edge effects, the three plants were chosen based on an even growth distribution and location; in other words, they were selected from the middle of the plot. The plants were divided into three parts (flower, leaf, and stem) and then put into the oven to cease metabolic activity (105 °C) for 30 min before being dried to a constant weight at 85 °C for measurement of dry biomass. The root samples within an area of 40 cm × 40 cm around the root were dug out by a spade from a 0–40 cm soil depth at the maturity stage of sunflower. All root samples were carefully washed and then dried to a constant weight using the same measurement of aboveground dry biomass. After measuring dry biomass, the dried plant samples were ground to 0.5 mm with an ultra-micro crusher (XL-30C, China). 50.0 mg plant samples were weighted and wrapped in tin foil cones, and then C content of each sample was determined by an element analyzer (Vario Macro CN, Germany).

2.2.3. Calculation of the net ecosystem carbon budget

The NECB was the difference between carbon input and carbon emission. In this study, the NECB was calculated as follows (Wu et al., 2018; Liu et al., 2019):

$$NECB = C_{input} - C_{output} = GPP + C_{amendment} - (R_c + R_s + C_h + CH_4) \quad (3)$$

$$\mathrm{GPP} = \mathrm{NPP} + R_c \quad (4)$$

$$\mathrm{NPP} = \mathrm{NPP}_f + \mathrm{NPP}_l + \mathrm{NPP}_s + \mathrm{NPP}_r \quad (5)$$

where *NECB* is net ecosystem carbon budget, t C ha^{-1}; *GPP* and *NPP* are gross primary production and net primary production, t C ha^{-1}, respectively, and the ratio of NPP/GPP is almost 0.52 (Wu et al., 2018); $C_{amendment}$ is the addition of C through application of LBF, t C ha^{-1}; R_c and R_s are respiration from crops and soil, respectively, t C ha^{-1}; C_h is carbon removed via harvest, t C ha^{-1}; and CH_4 is emissions of CH_4 from soil, t C ha^{-1}. NPP_f, NPP_l, NPP_s, and NPP_r are the net primary production of flowers, leaves, stems and roots of sunflower, respectively, which were determined by multiplying dry biomass and C content at sunflower harvest in this study, t C ha^{-1}. Considering that the organic carbon in the farmyard manure decomposes quickly in soil, while the organic carbon in the lignite decomposes slowly and exists in soil for a long time, only the $C_{amendment}$ of LBF was considered in this study.

2.2.4. Calculation of NGWP, NGWPI, and NEEB

To comprehensively evaluate the influence of FYM and LBF on global warming potential, the NGWP, net greenhouse gas intensity (NGWPI), and NEEB were calculated as follows (Wu et al., 2018; Liu et al., 2019):

$$\mathrm{NGWP} = 28 \times CH_4 + 265 \times N_2O + R_s - \frac{44}{12} \times (C_{amendment} + NPP) \quad (6)$$

$$\mathrm{NGWPI} = \mathrm{NGWP}/\mathrm{Y} \quad (7)$$

$$\mathrm{NEEB} = \mathrm{YB} - \mathrm{PC} - \mathrm{GWPC} \quad (8)$$

where *NGWP* is net global warming potential, with positive values indicating global warming potential (GWP) emissions from crop ecosystems and negative values indicating net sinks of GWP, t CO^2-equivalent ha^{-1}; CH_4, N_2O, and R_s are emissions of CH_4, N_2O, and CO_2, t ha^{-1}; *Y* is sunflower yield, t ha^{-1}; *NGWPI* is net greenhouse gas intensity (t t^{-1}); *NEEB* is the net ecosystem economic budget (thousand Chinese Yuan (CNY) ha^{-1}); *YB* is yield benefits, thousand CNY ha^{-1}; and *PC* and *GWPC* are the cost of planting and global warming potential, respectively, thousand CNY ha^{-1}. The price of GWP in the Chinese market is approximately 100 CNY per kg CO_2-equivalent.

2.2.5. Measurement of nitrogen and carbon cycling pathways

In this study, the primers 338F and 806R were used to amplify the 16S rRNA gene from bacteria (Bates et al., 2011). The details of soil DNA extraction and quality control of the raw 16S rRNA gene sequencing reads can be found in multiple previous studies (Magoč and Salzberg, 2011; Chen et al., 2018; Yang et al., 2021). To estimate the influence of FYM and LBF on nitrogen and carbon cycling, we focused on the functional gene families in nitrogen and carbon cycling processes. The gene of each operational taxonomic unit (OTU) was determined by PICRUSt2 software (Douglas et al., 2019). The gene families involved in nitrogen and carbon cycling were then selected using the Kyoto Encyclopedia of Genes and Genomes (KEGG) database. In this study, gene families involved in seven nitrogen cycling pathways, including nitrification, denitrification, assimilation, nitrogen fixation, ammonification, dissimilatory nitrate reduction, and assimilatory nitrate reduction, were compared among treatments, and a total of 47 modules for carbon cycling pathways were considered in this study.

2.3. Statical analysis

The differences in experimental variables were analyzed using R and DPS software by one-way analysis of variance (ANOVA). The least significant difference (LSD) method was used to determine the significant differences between values. Structural equation modeling (SEM) for evaluating the direct and indirect correlations between the soil properties and greenhouse gas emissions was performed in AMOS v.21.0 software (AMOS, IBM, USA). Structural equation modeling (SEM) was a comprehensive analysis including factor and pathway analyses. It was usually used to explore direct and indirect effects of independent variables on dependent variables, and to explore the importance of independent variables to dependent variables. In this study, we used SEM to explore the direct and indirect factors regulating the N_2O, CH_4, and CO_2 emissions, as well as to evaluate the contributions of these factors by assessing the degree of the standardized total effect (direct effect plus indirect effect). Models with a nonsignificant χ^2 test (ratio of Chi-Square to df (χ^2/df), $P > 0.05$), high goodness of fit index (GFI>0.90), and low root mean square error of approximation (RMSEA<0.05) were considered to be adequate.

3. Results

3.1. Soil greenhouse gas emission

Fig. 3 shows the dynamics of greenhouse gas emissions (CH_4, CO_2, and N_2O) during the growing period of sunflower in 2019 and 2020. As shown in Fig. 3A and B, in 2019 and 2020, CH_4 emissions of the FYM and CK treatments were generally higher than those of the LBF treatments (LBF1-LBF4). The highest CH_4 emissions were found in the FYM treatment in both 2019 and 2020. Specifically, CH_4 emissions of the FYM were in the ranges of −0.3 to 69.3 μg m^{-2} h^{-1} and -8.4 to 67.4 μg m^{-2} h^{-1}, respectively. The average CH_4 emissions of the CK treatment ranged from −5.9 to 89.1 μg m^{-2} h^{-1} and -18.4 to 62.5 μg m^{-2} h^{-1} in 2019 and 2020, respectively. Regarding the emissions of CO_2, Fig. 3C and D shows that the CO_2 emissions of the FYM and CK treatments were higher than those of the LBF treatments (LBF1-LBF4) in both 2019 and 2020. Specifically, compared with the CK treatment, the LBF treatments (LBF1-LBF4) reduced the average CO_2 emissions by 79.6–142.5 mg m^{-2} h^{-1} and 31.5–70.4 mg m^{-2} h^{-1} in 2019 and 2020, respectively, indicating that the application of LBF decreased CO_2 emissions. In addition, the FYM treatment increased the average CO_2 emissions by −59.7 and 19.8 mg m^{-2} h^{-1} in 2019 and 2020, respectively, compared to those in the CK treatment. For N_2O emissions, Fig. 3E and F illustrate that the N_2O fluxes of the FYM and LBF4 treatments were generally higher than those of the other treatments, especially after fertilizer application. The FYM treatment increased the average N_2O emissions by 5.1 and 142.2 μg m^{-2} h^{-1} in 2019 and 2020, respectively, compared to those in the CK treatment,

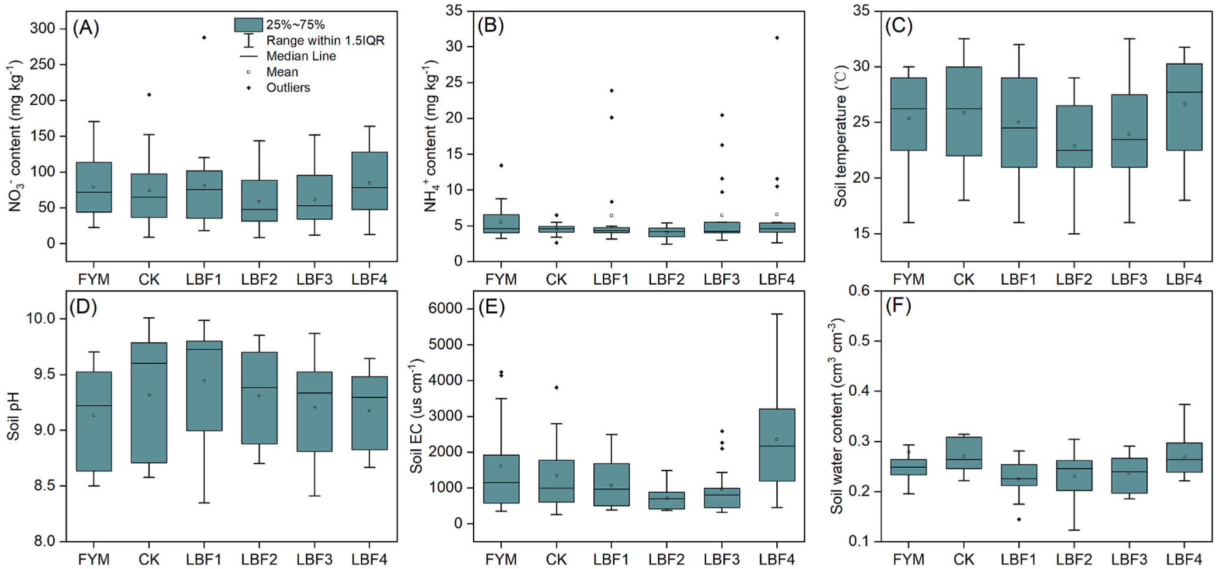

Fig. 2. Soil properties during sunflower growing period in 2019 and 2020.
Note: CK represents the control treatment without organic fertilizer; FYM is farmyard manure treatment applied with sheep manure of 21 t ha^{-1}; LBF1-LBF4 are four treatments applied with the lignite bioorganic fertilizer of 1.5, 3, 4.5 and 7.5 t ha^{-1}, respectively.

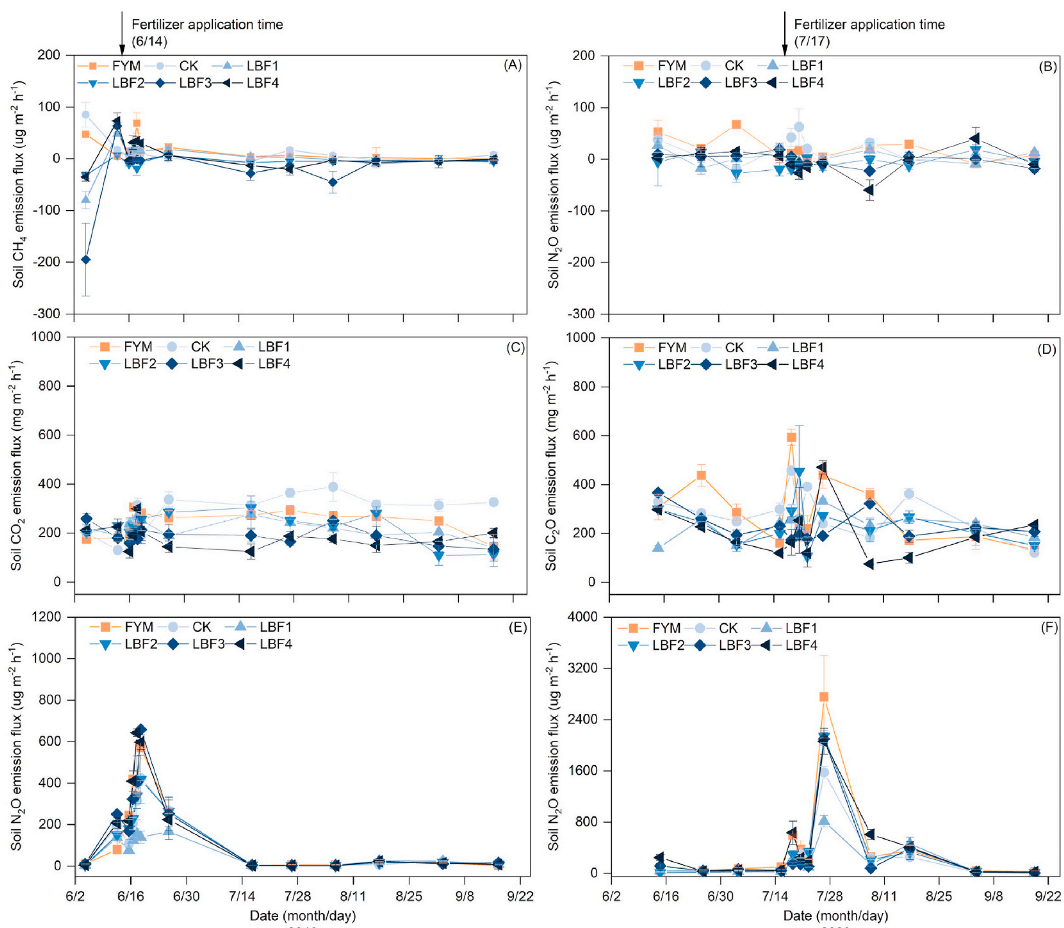

Fig. 3. The dynamics of greenhouse gas emissions (CH_4, CO_2, and N_2O) during the growing period of sunflower in 2019 and 2020.
Note: CK represents the control treatment without organic fertilizer; FYM is farmyard manure treatment applied with sheep manure of 21 t ha^{-1}; LBF1-LBF4 are four treatments applied with the lignite bioorganic fertilizer of 1.5, 3, 4.5 and 7.5 t ha^{-1}, respectively.

demonstrating that the application of FYM could augment N_2O emissions. In 2019, 2020, the average N_2O emissions of the LBF4 treatment were 9.2 and 132.0 μg m^{-2} h^{-1} higher than those of the CK treatment, respectively. It is worth noting that after the application of fertilizer (June 14, 2019 and July 17, 2020), the N_2O emissions of all treatments increased, especially those of the FYM, LBF3, and LBF4 treatments, while the CH_4 and CO_2 emissions rarely changed, indicating that the application of fertilizer only had a significant influence on N_2O emissions in saline-sodic soil.

The cumulative emissions of greenhouse gases (CH_4, CO_2, and N_2O) during the sunflower growth period in 2019 and 2020 are illustrated in Fig. 4. Fig. 4A and B shows that the FYM treatment increased the cumulative emissions of CH_4 by 0.05 and 0.25 kg ha^{-1}, respectively. In addition, the cumulative emissions of CH_4 in the FYM and CK treatments were both positive, making the FYM and CK treatments CH_4 sources. Compared with the CK treatment, the LBF treatments (LBF1-LBF4) decreased the cumulative emissions of CH_4, especially the LBF2 and LBF3 treatments, which decreased the cumulative emissions of CH_4 by 0.26 and 0.54 kg ha^{-1} in 2019 and by 0.29 and 0.22 kg ha^{-1} in 2020, respectively. Additionally, the cumulative emissions of CH_4 in the LBF2 and LBF3 treatments were negative, making the LBF2 and LBF3 treatments both CH_4 sinks. As shown in Fig. 4C and D, as the application rate of LBF increased, the cumulative emissions of CO_2 generally showed a decreasing trend. Compared with the CK treatment, the LBF1 to LBF4 treatments decreased the cumulative emissions of CO_2 by 1987.3–3557.6 kg ha^{-1} and 726.4–1668.8 kg ha^{-1} in 2019 and 2020, respectively, indicating that the application of LBF could decrease soil CO_2 emissions. Fig. 4E and F shows that compared with the CK treatment, the FYM treatment increased the cumulative emissions of N_2O, especially in 2020, in which the FYM treatment augmented the cumulative emissions of N_2O by 3.27 kg ha^{-1} in comparison with those in the CK treatment. Additionally, the cumulative emissions of N_2O in the LBF2 to LBF4 treatments were 0–0.35 kg ha^{-1} and 1.09–3.04 kg ha^{-1} in 2019 and 2020, respectively, which were higher than those in the CK treatment, suggesting that the application of LBF increased N_2O emissions when the application rate was over 3 t ha^{-1}.

The effects of soil chemistry properties on GHG emissions are clearly illustrated in Fig. 5. As shown in Fig. 5, the values of X^2/df, p, GFI, and RMSEA for the three SEMs indicated that the three SEMs met the significance criteria. Fig. 5A and E shows that the soil water content had the largest direct effect on CH_4 emissions, and the total effects of soil water content on CH_4 emissions were also the largest. As shown in Fig. 5B, CO_2 emissions were significantly positively affected by soil temperature and negatively affected by soil pH. Thus, the total effects of pH and soil temperature on CO_2 were greater than those of NH_4^+, EC, soil water content, and NO_3^- (Fig. 5F). Among all the studied soil chemistry properties, NH_4^+ and soil temperature significantly and positively affected N_2O emissions, while soil pH had a significantly negative influence on N_2O emissions (Fig. 5C). Soil temperature also indirectly affected N_2O emissions by impacting NH_4^+. NH_4^+, soil pH, and soil temperature generally had greater total effects on N_2O emissions than the other soil chemical properties. In addition, the total effect of soil pH on greenhouse gas emissions showed that soil pH negatively affected CH_4, CO_2, and N_2O emissions.

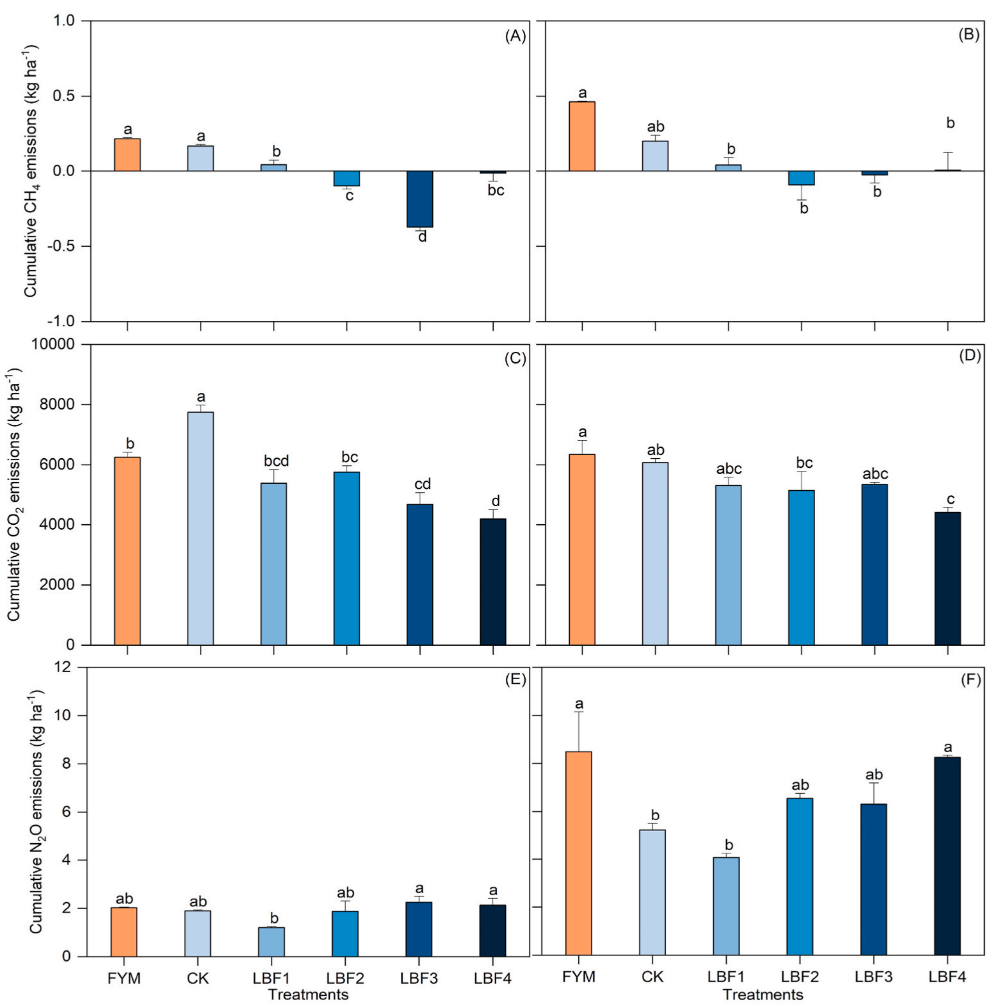

Fig. 4. The cumulative emissions of greenhouse gas (CH_4, CO_2, and N_2O) during the sunflower growth period in 2019 and 2020. Note: Different letters above the columns indicate significant difference at p < 0.05 level. CK represents the control treatment without organic fertilizer; FYM is farmyard manure treatment applied with sheep manure of 21 t ha-1; LBF1-LBF4 are four treatments applied with the lignite bio-organic fertilizer of 1.5, 3, 4.5 and 7.5 t ha^{-1}, respectively.

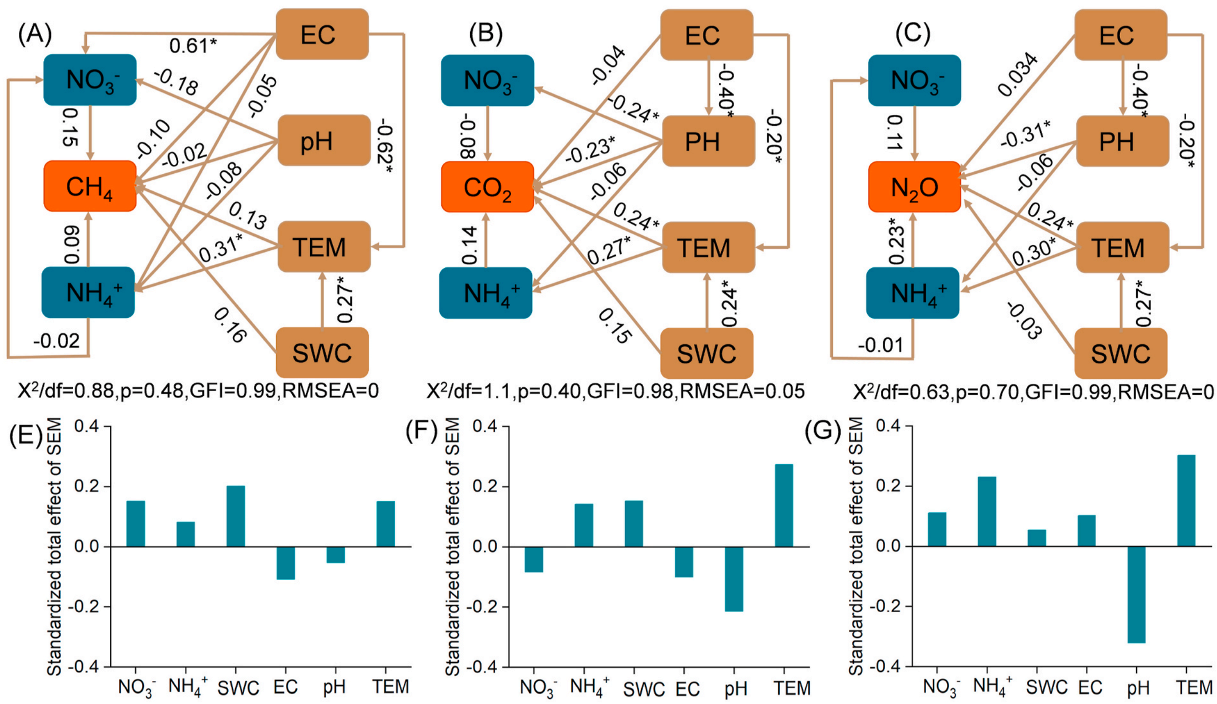

Fig. 5. Structure equation model for the standardized direct and indirect impacts of soil properties on greenhouse gas emissions (A-C) and the standardized total impacts on CH_4(D), CO_2(E), and N_2O(F).
Note: The numbers in the A-C represent the standardized direct impacts on greenhouse gas emissions. The black asterisk means that the effects are significant at $p < 0.05$ level. EC, TEM, and SWC are soil electricity conductivity, soil temperature, and soil water content, respectively. CK represents the control treatment without organic fertilizer; FYM is farmyard manure treatment applied with sheep manure of 21 t ha^{-1}; LBF1-LBF4 are four treatments applied with the lignite bioorganic fertilizer of 1.5, 3, 4.5 and 7.5 t ha^{-1}, respectively.

Table 2
The net ecosystem carbon budget and its components in 2019 and 2020.

Year	Treatment	NPP (t ha^{-1})	$C_{amendment}$ (t ha^{-1})	C_h (t ha^{-1})	C_s (t ha^{-1})	NCEB (t ha^{-1})
	FYM	6.01 ± 0.64b	0.00	2.35 ± 0.18b	1.71 ± 0.03b	1.95 ± 0.74d
	CK	3.85 ± 0.05c	0.00	1.57 ± 0.19c	2.11 ± 0.04a	0.17 ± 0.11e
	LBF1	5.93 ± 0.37b	0.52	2.49 ± 0.16b	1.47 ± 0.07bcd	2.49 ± 0.4c
2019	LBF2	8.16 ± 0.37a	1.04	3.19 ± 0.32a	1.57 ± 0.03bc	4.45 ± 0.71bc
	LBF3	9.48 ± 0.47a	1.56	3.55 ± 0.2a	1.27 ± 0.06cd	6.21 ± 0.29a
	LBF4	5.31 ± 0.29bc	2.60	1.51 ± 0.32c	1.140.05d	5.26 ± 0.11 ab
	FYM	4.04 ± 0.3cd	0.00	1.66 ± 0.04bc	1.73 ± 0.07a	0.65 ± 0.42c
	CK	3.32 ± 0.2d	0.00	1.15 ± 0.12d	1.66 ± 0.02 ab	0.52 ± 0.34c
	LBF1	3.57 ± 0.12d	0.52	1.45 ± 0.05cd	1.45 ± 0.04abc	1.2 ± 0.16b
2020	LBF2	6.21 ± 0.1b	1.04	2.03 ± 0.05 ab	1.4 ± 0.1bc	3.81 ± 0.12a
	LBF3	7.34 ± 0.19a	1.56	2.11 ± 0.2a	1.46 ± 0.01abc	5.34 ± 0.06a
	LBF4	4.66 ± 0.12c	2.60	1.13 ± 0.09d	1.20.03c	4.93 ± 0.24a

Note: Values in table are mean ± standard deviation; Different letters in same column indicate significant difference at $p < 0.05$; NPP, $C_{amendment}$, C_h, C_s, and NCEB are net primary production, addition C through application of LBF, removed carbon from harvest, carbon output from soil (CO_2 and CH_4), and net ecosystem carbon budget, respectively; CK represents the control treatment without organic fertilizer; FYM is farmyard manure treatment applied with sheep manure of 21 t ha^{-1}; LBF1-LBF4 are four treatments applied with the lignite bioorganic fertilizer of 1.5, 3, 4.5 and 7.5 t ha^{-1}, respectively.

3.2. Net ecosystem carbon budget and global warming potential

The components of the net ecosystem carbon budget in 2019 and 2020 are listed in Table 2. The NPP first increased and then decreased with the increase in the application rate of LBF. The highest NPPs obtained in the LBF3 treatment were 9.48 and 7.34 t ha^{-1} in 2019 and 2020, respectively. The LBF treatments increased the NPP by 0.72–5.63 and 0.25 to 4.02 t ha^{-1} in 2019 and 2020, respectively, in comparison with that in the CK treatment, indicating that the application of LBF could increase net primary productivity, especially the application of LBF at 4.5 t ha^{-1}. The NPP of the FYM treatment was 2.16 and 0.72 t ha^{-1} higher than that of the CK treatment in 2019 and 2020, respectively. Overall, the application of LBF and FYM increased net primary productivity. Additionally, compared with the FYM treatment, the LBF3 treatment significantly increased the NPP by 57.7% and 81.7% in 2019 and 2020, respectively. The carbon output in harvested grain (C_h) was also increased by the FYM and LBF treatments, except for the LBF4 treatment. Compared with the CK treatment, the LBF1 to LBF3 treatments obviously increased C_h by 0.92–1.98 and 0.3 to 0.96 t ha^{-1} in 2019 and 2020, respectively. The C_h of the FYM treatment was 0.78 and 0.51 t ha^{-1}, which was significantly higher than that of the CK treatment in 2019 and 2020, respectively. In contrast, the application of LBF decreased the carbon output (C_s) from soil (CO_2 and CH_4), and C_s generally showed a decreasing trend as the application rate of the LBF increased in both 2019 and 2020. The LBF treatments decreased the C_s by 0.54–0.97 t ha^{-1} and 0.2 to 0.46 t ha^{-1} in 2019 and 2020, respectively, compared with those in the CK treatment. Moreover, the C_s in the FYM treatment was also 0.14 to 0.57 t ha^{-1} and 0.27 to 0.53 t ha^{-1} higher than that of the LBF treatments in 2019 and 2020, respectively. Overall, the CK treatment, with the lowest carbon sequestration in plants and the highest carbon output from the soil, had the lowest net ecosystem carbon budget (NCEB). Compared with the CK treatment, the FYM treatment increased NCEB by 1.78 and 0.07 t ha^{-1} in 2019 and

2020, respectively. Additionally, as the application rate of LBF increased, the NCEB first increased and then decreased. Among all the treatments, the LBF3 treatment had the highest NCEB, which was 6.04 and 4.82 t ha^{-1} higher than that in the CK treatment in 2019 and 2020, respectively. It is worth noting that the NCEB in the CK treatment was positive, making the CK treatment a carbon sink.

Next, considering that compared with the CK treatment, the LBF3 treatment significantly improved the NCEB and the FYM treatment was a positive control, the carbon budgets in the CK, FYM, and LBF3 were compared further (Fig. 6). As shown in Fig. 6, compared with the CK treatment, the LBF3 treatment increased the average carbon stock in the flowers, leaves, stems, and roots of sunflower by 2.26, 0.66, 1.33, and 0.58 t ha^{-1} across the two experimental years, respectively, which were all higher than those in the FYM treatment. In general, the average gross primary production (GPP_0) and respiration (R_0) for the crop ecosystem were both improved by the LBF3 and FYM treatments. However, the increased GPP_0 and R_0 in the LBF3 treatment were significantly higher than those in the FYM treatment.

The GWP, NGWP, yield, NGWPI, and NEEB of the treatments are listed in Table 3 to further show the effects of LBF and FYM on the environment and net ecosystem economic budget. Compared with the CK treatment, the LBF treatments decreased the GWP by 2.33–4.41 t ha^{-1} and 0.58 to 1.07 t ha^{-1} in 2019 and 2020, respectively. The NGWP values of all treatments were negative, indicating that all treatments in this study reduced the global warming potential. The LBF3 treatment had the lowest NGWP value, which was 22.09 and 17.39 t ha^{-1} lower than that in the CK treatment in 2019 and 2020, respectively. The NGWPI decreased as the application rate of LBF increased. As the application rate of LBF increased, the NEEB first increased and then decreased, and the highest NEEB was found in the LBF3 treatment in 2019 and in the LBF2 treatment in 2020, which was 8.81 and 6.01 thousand CNY ha^{-1} significantly higher than that in the CK treatment in 2019 and 2020, respectively. Although the FYM treatment decreased the NGWP, it reduced the NEEB by 2.69 and 7.84 thousand CNY ha^{-1} in comparison with that in the CK treatment. In addition, compared with the application of farmyard manure, applying lignite bioorganic fertilizer at 3.0–4.5 t ha^{-1} significantly improved net ecosystem carbon budget, net global warming potential, and net ecosystem economic budget by 2.5–4.7 t ha^{-1}, -17.8 to −9.2 t CO_2 ha^{-1}, and 10.3–12.9 thousand CNY ha^{-1}, respectively. Overall, the application of LBF at 3 to 4.5 t ha^{-1} could significantly increase the NEEB.

3.3. N cycling pathways

To further study the effects of LBF and FYM on nitrogen cycling pathways, the relative abundance of genes for seven pathways of nitrogen cycling was compared in this study. Considering that the LBF3 treatment had the highest NCEB and that the FYM treatment was a positive control treatment, only the gene abundance of nitrogen cycling pathways in the CK, FYM, and LBF3 treatments was further compared (Fig. 7).

As shown in Fig. 7A, for the nitrogen fixation process, the LBF3 and FYM treatments significantly increased the relative abundance of *nifDKH* by 17.6% and 94.7%, respectively, in comparison with that in the CK treatment, indicating that the LBF3 and FYM treatments increased the reduction of N_2 to crop available NH_4^+.

For the nitrification process, compared with the CK treatment, the LBF3 and FYM treatments significantly increased the relative abundance of gene families encoding NH_4^+ to NH_2OH conversion (*amoABC*) and reduced the relative abundance of those associated with NH_2OH to NO_2^- conversion (*hao*). Additionally, the LBF3 and FYM treatments increased the abundance of *nxrAB* genes involved in converting NO_2^- to NO_3^- by 4.6% and 20.5%, respectively, compared with that in the CK treatment.

For the denitrification process, the LBF3 treatment obviously increased the abundance of the *narGHI* (NO_3^- to NO_2^-), *nirKS* (NO_2^- to NO), *norBC* (NO to N_2O), and *nosZ* (NO_2^- to NO) gene families by 3.3%, 13.0%, 2.7%, and 9.0%, respectively, in comparison with that in the CK treatment. Compared with the CK treatment, the FYM treatment improved the abundance of the *narGHI* and *napAB* gene families by 20.7% and significantly reduced the abundance of the *nirKS*, *norBC*, and *nosZ* gene families by 20.7%, 14.7%, and 11.0%, respectively. Overall,

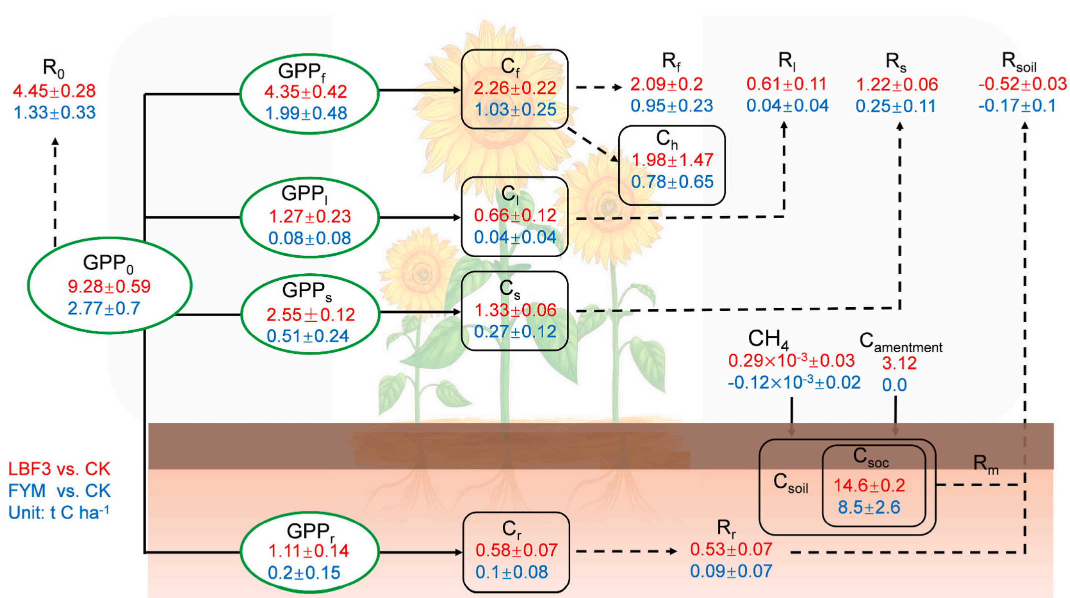

Fig. 6. Carbon budget changes under application of farmyard manure and lignite bioorganic fertilizer in a saline-sodic soil with sunflower production.
Note: The values are calculated as (value in the treatment with application of farmyard manure or the lignite bioorganic fertilizer with 4.5 t ha^{-1} minus value in the control treatment). Oval-shaped boxes is gross primary production for crop ecosystem (GPP_0), flower (GPP_f), leaf (GPP_l), stem (GPP_s), and root (GPP_r), respectively. Square-shaped boxes are average carbon stocks in two experimental years, such as flower (C_f), leaf (C_l), stem (C_s), root (C_r), soil (C_{soil}), soil organic carbon (C_{soc}) and harvest yield (C_h), respectively. Unboxed variables are carbon fluxes, including emissions of CH_4, amendment C ($C_{amendment}$), total respiration of crop ecosystem (R_0) and respiration of flower (R_f), leaf (R_l), stem (R_s), root (R_r), microbe (R_m), and soil (R_{soil}), respectively.CK represents the control treatment without organic fertilizer. FYM is farmyard manure treatment applied with sheep manure of 21 t ha^{-1}. LBF3 is treatments applied with the lignite bioorganic fertilizer of 4.5 t ha^{-1}.

Table 3
The global warming potential, net global warming potential, net global warming potential intensity, and net ecosystem economic budget in 2019 and 2020.

Yield	Treatment	GWP (t CO_2 ha $^{-1}$)	Yield (t ha $^{-1}$)	NGWP (t CO_2 ha $^{-1}$)	NGWPI (t t $^{-1}$)	NEEB (Thousand CNY ha $^{-1}$)
2019	FYM	6.8 ± 0.19b	3.1 ± 0.4b	−6.62 ± 3.3bc	−2.29 ± 1.21bc	10.04 ± 2.17c
	CK	8.25 ± 0.29a	2 ± 0.4c	−0.1 ± 0.48c	−0.12 ± 0.24c	12.73 ± 2.27bc
	LBF1	5.71 ± 0.56bcd	3.1 ± 0.3b	−8.81 ± 1.81b	−2.91 ± 0.74bc	18.29 ± 1.78 ab
	LBF2	6.25 ± 0.33bc	4 ± 0.7a	−15.81 ± 3.3a	−4.32 ± 1.53b	21.5 ± 3.65a
	LBF3	5.26 ± 0.42cd	4.5 ± 0.4a	−22.19 ± 1.29a	−4.94 ± 0.07b	21.54 ± 2.67a
	LBF4	4.75 ± 0.3d	1.9 ± 0.7c	−18.71 ± 0.39a	−11.16 ± 2.64a	−8.55 ± 3.9d
2020	FYM	8.61 ± 0.98a	2.7 ± 0.1bc	−0.13 ± 1.82c	−0.03 ± 0.67d	6.23 ± 0.77c
	CK	7.46 ± 0.08 ab	2 ± 0.4c	−0.51 ± 1.2c	−0.45 ± 0.7d	13.07 ± 1.86b
	LBF1	6.39 ± 0.34b	2.8 ± 0.2b	−3.31 ± 0.61c	−1.21 ± 0.24cd	14.73 ± 0.85 ab
	LBF2	6.88 ± 0.78b	3.8 ± 0.2a	−12.24 ± 0.49b	−3.28 ± 0.21bc	19.08 ± 0.86a
	LBF3	7.02 ± 0.3b	3.9 ± 0.6a	−17.9 ± 0.06a	−4.67 ± 0.38b	16.49 ± 3.57 ab
	LBF4	6.59 ± 0.2b	2.1 ± 0.3bc	−15.89 ± 0.88 ab	−7.63 ± 0.92a	−6.93 ± 1.5d

Note: Values in table are mean ± standard deviation; Different letters in same column indicate significant difference at $p < 0.05$; GWP, NGWP, NGWPI, and NEEB are global warming potential, net global warming potential, net global warming potential intensity, and net ecosystem economic budget, respectively. CK represents the control treatment without organic fertilizer; FYM is farmyard manure treatment applied with sheep manure of 21 t ha^{-1}; LBF1-LBF4 are four treatments applied with the lignite bioorganic fertilizer of 1.5, 3, 4.5 and 7.5 t ha^{-1}, respectively; CNY is Chinese Yuan.

the denitrification process was improved by the LBF3 treatment and limited by the FYM treatment.

For nitrate reduction processes (dissimilatory (DNRA) and assimilatory (ANRA) processes), the LBF3 and FYM treatments had a similar impact on the abundance of gene families involved in the conversion of NO_3^- to NH_4^+. Specifically, the LBF3 treatment increased the abundance of the *narGHI* and *napAB* (NO_3^- to NO_2^- in DNRA), *nrfAH* and *nirAB* (NO_2^- to NH_4^+ in DNRA), and *narA* and *nasAB* (NO_3^- to NO_2^- in ANRA) gene families, while only the *nirA* (NO_2^- to NH_4^+ in ANRA) gene families were reduced in the LBF3 treatment. The application of FYM improved all gene families involved in nitrate reduction processes. Generally, the nitrate reduction processes, both DNRA and ANRA, were improved by applying FYM and LBF.

For the assimilation process, the gene families encoding the conversion of NH_4^+ to organic nitrogen (*glnA*, *gltBD*, and *GLU*) were improved by 3.7% and 1.5% by LBF3 and FYM, respectively, in comparison with those in the CK treatment. For ammonification, the total relative abundance of the *ureC*, *nitrilase*, and *formamidase* gene families in the LBF3 and FYM treatments was 10.2% and 10.5% higher than that in the CK treatment, indicating that the application of LBF and FYM improved the ammonification of organic nitrogen.

3.4. C cycling pathways

There are 47 modules in carbon cycling pathways, according to KEGG datasets. However, only the average relative abundance of the acetyl-CoA pathway involved in the methane oxidation process was lower than 0.01%. Thus, a total of 46 modules for carbon cycling among the FYM, LBF3, and CK treatments were analyzed in this study. As shown in Fig. 8, 46 modules in the carbon cycling pathways could be grouped into six subgroups: carbohydrate metabolism, carbon fixation in photosynthetic organisms (CFPO), carbon fixation pathways in prokaryotes (CFPP), methanogenesis, methane oxidation, and amino acid metabolism. Carbohydrate metabolism included a total of 21 modules, half of which (from glycolysis to propanoyl-CoA metabolism in Fig. 8) were improved by the LBF3 treatment and the other half of which (from pentose phosphate pathway to malonate semialdehyde pathway in Fig. 8) were reduced by the LBF3 treatment in comparison with those in the CK treatment. In general, the total relative abundance of all modules involved in carbohydrate metabolism in the LBF3 treatment was 8.9% lower than that in the CK treatment. In addition, the difference in the total relative abundance modules for carbohydrate metabolism between the FYM and CK treatments was minimal. For carbon fixation, the abundance of modules in CFPO was increased by the LBF3 and FYM treatments. In contrast, the abundance of modules in CFPP was reduced by those two treatments, indicating that the application of LBF and FYM could increase photosynthetic organisms in the soil. In general, the effects of LBF and FYM on carbon fixation were not significant. For modules of the methanogenesis process, compared with the CK

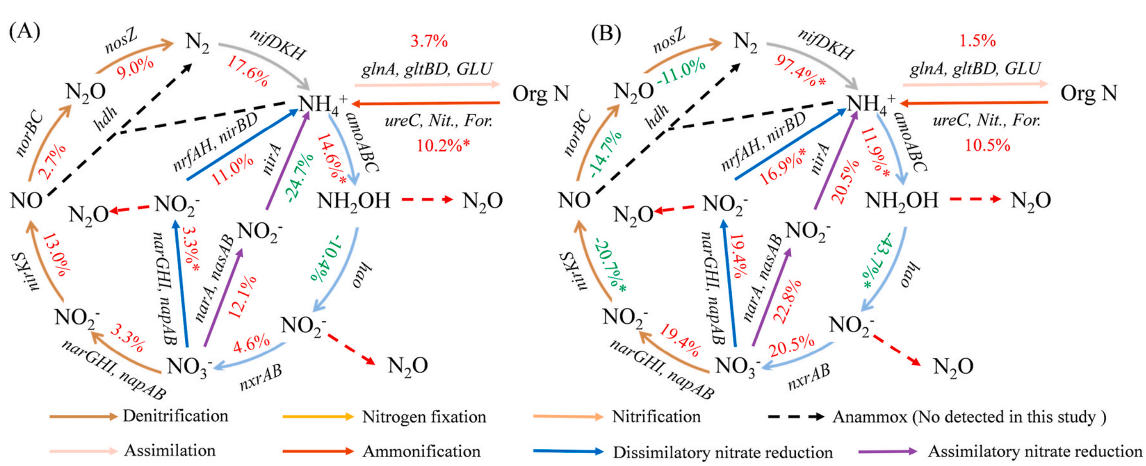

Fig. 7. Percentage changes in nitrogen cycling gene families between the control treatment and the treatment with application of lignite bioorganic fertilizer with 4.5 t ha^{-1} (A) or farmyard manure (B).
Note: The values are calculated as (value in the treatment with application of the lignite bioorganic fertilizer with 4.5 t ha^{-1} (A) or farmyard manure (B)/value in the control treatment - 1) × 100. The black asterisk means that the effects are significant at $p < 0.05$ level. The italics are names of gene families.

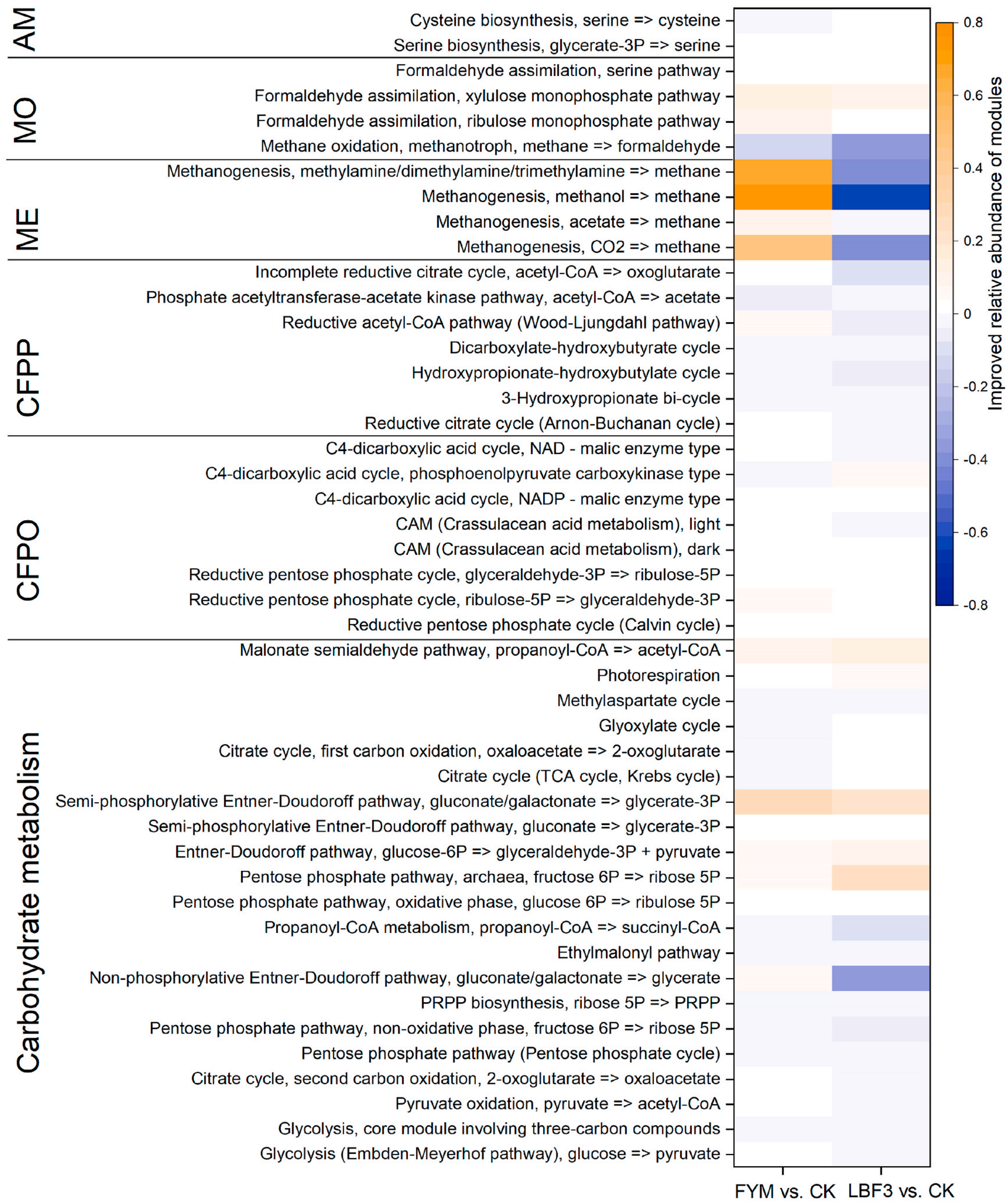

Fig. 8. Changes in carbon cycling gene families compared with the control treatment.
Note: CFPO, CFPP, ME, MO, and AM are carbon fixation in photosynthetic organisms, carbon fixation pathways in prokaryotes, methanogenesis, methane oxidation, and amino acid metabolism processes, respectively. FYM and LBF3 are the treatments with application of the lignite bioorganic fertilizer with 4.5 t ha^{-1} and farmyard manure, respectively.

treatment, the LBF3 treatments reduced the abundance by 11.0%, while the FYM treatment improved the abundance by 18.5%. For the abundance of modules of methane oxidation, the FYM and LBF3 treatments improved the abundance by 4.5 and 2.2%, respectively. For amino acid metabolism (AMM) modules, the LBF and FYM treatments slightly improved abundance compared with that in the CK treatment.

4. Discussion

4.1. Effects of lignite bioorganic fertilizer and farmyard manure on GHG

Previous studies have widely recognized that organic amendments, such as farmyard manure and organic fertilizer, influence CH_4, CO_2, and N_2O emissions directly by carbon and nitrogen compounds present in these organic fertilizers and indirectly by impacting soil properties (Li et al., 2020; Shakoor et al., 2021a). In this study, the application of FYM (sheep manure) increased the CH_4 emission rate during the sunflower growth period. It thus improved the total emissions of CH_4 by 0.05 and 0.25 kg ha^{-1} in 2019 and 2020, respectively, in comparison with those in the CK treatment. This result was consistent with the result of Shakoor et al. (2021b), who reported that the application of manure fertilizer considerably increased CH_4 emissions on the basis of a meta-analysis. Similarly, Pathak (2015) also proved that amendments of manure fertilizer could significantly enhance CH_4 emissions. In contrast, the application of LBF significantly decreased CH_4 emissions in both 2019 and 2020 compared with those in the CK treatment, and the application of LBF even made soil act as a CH_4 sink for some treatments. This result was similar to that of Li et al. (2020), who found that LBF amendments decreased CH_4 emissions in an incubation experiment. Many studies have proven that CH_4 is mainly emitted under anaerobic conditions (Praeg et al., 2016; Li et al., 2020; Shakoor et al., 2021b). In this study, the effect of the soil properties on the CH_4 emissions was further explored using SEMs. The results showed that the soil water content had a positive impact on the CH_4 emissions, and the total effect of soil water content on the CH_4 emissions was the largest. Therefore, the FYM treatment increased the CH_4 emissions mainly because the FYM treatment had a higher soil water content (Fig. 5), which resulted in stricter anaerobic conditions than the other treatments. In addition, the application of FYM also improved the growth of crops and increased the consumption of oxygen, which also caused anaerobic conditions for methanogenesis (Thangarajan et al., 2013). The reason for the lower CH_4 emissions in the LBF treatments was probably that the application of LBF increased soil porosity, which limited the process of methanogenesis and improved the process of methane oxidation (Fig. 8).

Emissions of CO_2 from croplands were mainly due to soil microbial and crop root respiration (Ray et al., 2020). In previous studies, CO_2 emissions from croplands were improved by applying animal manure mainly because animal manure provided organic carbon that increased the respiration of microbial communities (Watts et al., 2011; Li et al., 2021; Bore et al., 2017). However, in this study, compared with the CK treatment, the FYM treatment significantly decreased CO_2 emissions in 2019, and the difference in CO_2 emissions between the FYM and the CK treatments was marginally noticeable in 2020. These different results might be caused by the application rate of FYM and soil physicochemical properties (Shakoor et al., 2021a). In addition, compared with the CK treatment, the LBF treatments reduced total CO_2 emissions by 1987.3–3557.6 kg ha^{-1} and 726.4–1668.8 kg ha^{-1} in 2019 and 2020, respectively. Li et al. (2020) also found that the application of LBF limited CO_2 emissions. This result was also consistent with that of Tran et al. (2015), who reported that the application of lignite decreased the emissions of CO_2. The SEM results showed that the soil temperature had the largest positive effects on CO_2 emissions (Fig. 5), and lower soil temperatures were obtained in the LBF treatments, except for the LBF4 treatment. The reason for the lower soil temperature in the LBF2 and LBF3 treatments was that the application of LBF improved sunflower growth (except for the LBF4 treatment), which caused more shadowing of the soil. Therefore, the reason for the lower CO_2 emissions in the LBF treatments (except for the LBF4 treatment) is probably that the lower soil temperature suppressed soil respiration. In addition, the LBF4 treatment overused lignite bioorganic fertilizer, resulting in an increase in soil electrical conductivity. Therefore, the mainly reason for the negative effects of LBF4 on CO_2 emissions was probably that LBF4 increased soil salinity that suppressed CO_2 emissions.

The impact of farmyard manure on soil N_2O emissions varied widely among individual studies. Li et al. (2020) reported that the application of FYM had little influence on N_2O emissions. However, Shakoor et al. (2021a) found that the addition of FYM significantly increased N_2O emissions. Similarly, in this study, the application of FYM increased N_2O emissions, especially in 2020. In this study, to further study the impact of soil properties on N_2O emissions, an SEM was established to explore the relationships between N_2O emissions and soil properties. The results showed that NH_4^+ content, soil temperature, and soil pH had a greater effect on N_2O, indicating that these were the main factors that influenced N_2O emissions. Additionally, the NH_4^+ in the FYM treatment was higher than that in the CK treatment (Fig. 2). Therefore, the reason for the higher N_2O emissions in the FYM treatment was probably that the application of FYM increased the soil NH_4^+ for the nitrification process and subsequently N_2O emissions (Hayakawa et al., 2009). This result was consistent with those of Zhou et al. (2017) and Guenet et al. (2021), who reported that FYM increased N_2O emissions due to decomposable SOC provided by FYM, which could improve soil N mineralization and then increase the production of N_2O. For the effects of LBF on N_2O emissions, in this study, the application of LBF increased N_2O emissions when the application rate was over 3 t ha^{-1}. This result was consistent with the findings of Li et al. (2020), who also reported that N_2O increased with an increase in the application rate of LBF. The potential reasons for this result were mainly that the addition of LBF improved the NH_4^+ content that provided sufficient substrate nitrification processes (Thangarajan et al., 2013; Li et al., 2020). However, Fig. 2 shows that the NH_4^+ content in the LBF treatments was not obviously higher than that in the CK treatment. The reason for this result was probably that the sunflower growth and emissions of N_2O in the LBF treatments consumed more NH_4^+ than those in the CK treatment.

Additionally, previous studies exploring the effect of FYM and LBF on N_2O emissions at the gene level are scarce. In this study, to further study the mechanism at the gene level for the effects of FYM and LBF on N_2O emissions, the abundance of gene families in four main processes (nitrification, denitrification, nitrifier denitrification, and DRNA) that could cause N_2O emissions was compared among treatments. The results showed that the first step of nitrification (from NH_4^+ to NH_2OH) was improved by applying LBF and FYM. This result was also evidence that the application of FYM and LBF improved the NH_4^+ content and then increased the nitrification processes and subsequently N_2O production. In this study, the results also showed that the abundance of *hao* (NH_2OH to NO_2^-) was reduced by amendment with FYM and LBF, which caused the accumulation of NH_2OH and then increased N_2O emissions. Moreover, the LBF3 treatment improved the abundance of *norBC* (NO to N_2O), while the FYM treatment reduced it in comparison with that in the CK treatment. Additionally, the DNRA process was increased by applying LBF and FYM, which probably increased N_2O emissions. Overall, the reason for the increase in N_2O emissions in the FYM treatment was mainly that the application of FYM limited the second step of nitrification (NH_2OH to NO_2^-) and improved the process of DNRA. The N_2O emissions increased in response to the LBF3 treatment mainly because the application of LBF not only limited the pathway of NH_2OH to NO_2^- in the nitrification process but also increased the pathway of NO to N_2O in the denitrification process and improved the DNRA process.

4.2. *Effects of lignite bioorganic fertilizer and farmyard manure on the soil carbon budget*

Generally, in this study, the LBF treatments decreased the GWP by 5.9–14.3% and 24.2–42.4% in 2019 and 2020, respectively, indicating that the application of LBF could alleviate the GWP. Additionally, FYM addition increased the GWP in 2019 and decreased the GWP in 2020. The different precipitation and air temperatures in the two experimental years probably caused these opposite results in the two experimental years.

Although many previous studies were conducted to evaluate the effect of organic additions on global warming potential (Yang et al., 2020; Shakoor et al., 2021b), very few studies were conducted to investigate the impact of the application of organic amendments on the carbon budget and net global warming potential. Actually, it is questionable whether the influence of organic amendment on the global warming potential was simply evaluated by greenhouse gas emissions from the soil because at the same time as greenhouse gas emitted from the soil, the cropping systems acted as the carbon sink through crop photosynthesis (Liu et al., 2019). Instead, the net ecosystem carbon budget (NECB), net global warming potential (NGWP), and net ecosystem economic budget (NEEB) could comprehensively reflect the impact of the application of organic amendments on global warming potential and environmental profits. In this study, the NECB was increased by applying FYM and LBF, indicating that FYM and LBF amendments could make more carbon sinks in the soil and subsequently alleviate global warming potential. Among the LBF treatments, the LBF3 treatment had the highest NECB value in both 2019 and 2020, indicating that the application of LBF at 4.5 t ha^{-1} can be recommended to increase the carbon budget in the cropping system. It is worth noting that the NECB in the CK treatment was positive, showing that the CK treatment was a carbon sink. There are two probable explanations for this result. On the one hand, greenhouse gas emissions from saline-sodic soil are significantly restricted compared with those from normal farmland (Yang et al., 2021). On the other hand, optimal agronomic practices, such as irrigation before seeding and chemical fertilizer input, increased crop growth and carbon assimilation by crop photosynthesis. This result was consistent with the findings of Yang et al. (2021), who reported that optimal agronomic practices could change the carbon source to a carbon sink in saline-sodic farmland. Similarly, the NGWP also decreased in response to the FYM and LBF treatments, suggesting that the application of FYM and LBF could make saline-sodic farmland a greenhouse gas sink, especially the application of LBF at 4.5 t ha^{-1}.

In this study, there was no significant difference in the NEEB between the LBF2 and LBF3 treatments, indicating that the application of LBF at 3.0 to 4.5 t ha^{-1} could obtain the largest net ecosystem economic profits. Additionally, the NEEB of the LBF4 treatment was negative, indicating that overuse of LBF resulted in a loss of net ecosystem economic profits. The NEEB of the FYM treatment was even lower than that of the CK treatment. This result was mainly because increased profits from FYM treatment could not offset the cost of FYM. In summary, the application of LBF at 3.0 to 4.5 t ha^{-1} was is recommended for saline-sodic farmland to improve the NEEB in the Hetao Irrigation District.

4.3. Effects of lignite bioorganic and farmyard manure on N cycling and C cycling

Previous studies have consistently evaluated the influence of organic amendments on soil GHG emissions (Agegnehu et al., 2016; Abagandura et al., 2019), but very few studies have been conducted to explore how the application of organic amendments impacts N and C cycling pathways. In this study, we identified the impacts of FYM and LBF on the abundance of functional genes involved in N cycling pathways. Overall, the difference in functional gene abundance for N cycling between the CK and LBF3 treatments showed that all functional gene abundances were improved by the LBF3 treatment, except for the abundances of *nirA* and *hao*. This result was probably because the application of LBF at 4.5 t ha^{-1} alleviated soil salinity (Fig. 2) and then reduced the limitation of salinity on gene abundance (Yang et al., 2021; Rath et al., 2018; Zhao et al., 2020). Notably, the increased gene families involved in the denitrification and nitrate reduction processes could reduce nitrate leaching and increase NH_4^+ content. Additionally, the increased gene families involved in the ammonification process could also improve NH_4^+ content. These three processes improve inorganic N availability for crop growth (Schwaner and Kelly, 2019; Kelly et al., 2021). This result probably explained why the NPP in the LBF3 treatment was the largest (Fig. 6). Similarly, compared with the CK treatment, the FYM treatment also improved the abundance of genes involved in assimilation, ammonification, nitrification, and nitrate reduction, indicating that the application of FYM could improve NH_4^+ for crop growth. However, the FYM treatment decreased the gene families involved in the process of denitrification. In general, the performance of LBF3 for improving N cycling gene abundance was better than that of the FYM treatment.

All modules involved in carbon cycling were evaluated in this study. The results showed that, in general, modules for carbohydrate metabolism in the LBF3 treatment were lower than those in the CK treatment, indicating that the application of LBF limited the carbohydrate metabolism process. This result was similar to the result of Li et al. (2020). This result also explained why lower CO_2 emissions were found in the LBF treatments. Notably, modules in CFPO were increased by the application of LBF, while the abundance of modules in CFPP was reduced, indicating that the application of LBF could improve photosynthetic organisms in the soil. Moreover, the LBF treatments reduced the modules of methanogenesis, while the FYM treatment increased the modules of methanogenesis. This result also explained why lower CH_4 emissions were obtained in the LBF treatments than in the FYM treatment (Wang et al., 2019; Qi et al., 2020).

5. Conclusion

In conclusion, to the best of our knowledge, this work represents one of the first studies to estimate the influence of farmyard manure and lignite bioorganic fertilizer on the net ecosystem carbon budget, net global warming potential, and nitrogen and carbon cycling pathways in saline-sodic farmlands. The application of lignite bioorganic fertilizer significantly decreased the emissions of CH_4 and CO_2 while increasing N_2O emissions. We found evidence that the application of lignite bioorganic fertilizer reduced the soil water content and limited the gene families related to methanogenesis, thus decreasing CH_4 emissions. The modules in carbohydrate metabolism were reduced in the treatment with the addition of lignite bioorganic fertilizer. This result was probably the main reason for the reduced CO_2 emissions in treatments with lignite bioorganic fertilizer. Lignite bioorganic fertilizer improved the soil NH_4^+ content, which had a positive relationship with N_2O emissions. Additionally, the application of lignite bioorganic fertilizer increased the abundance of *norBC* genes and gene families involved in dissimilatory nitrate reduction and decreased *hao* gene abundance, thus triggering the emissions of N_2O. The application of lignite bioorganic fertilizer significantly improved the net ecosystem carbon budget. This made the treatments a net global warming potential sink, especially when applying lignite bioorganic fertilizer at 3.0–4.5 t ha^{-1}. Ultimately, the net ecosystem economic budget was obviously improved by 21.5 and 17.8 thousand CNY ha^{-1} in 2019 and 2020, respectively, with the application of lignite bioorganic fertilizer at 3.0–4.5 t ha^{-1}. In 2019, 2020, although the addition of farmyard manure also improved the net ecosystem carbon budget by 1.78 and 0.13 t ha^{-1} in comparison with the CK treatment, it decreased the net ecosystem economic budget by 2.69 and 6.83 thousand CNY ha^{-1}, respectively. In addition, compared with the application of farmyard manure, applying lignite bioorganic fertilizer at 3.0–4.5 t ha^{-1} significantly improved net ecosystem carbon budget, net global warming potential, and net ecosystem economic budget by 2.5–4.7 t ha^{-1}, -17.8 to −9.2t CO_2 ha^{-1}, and 10.3–12.9 thousand CNY ha^{-1}, respectively. In conclusion, the application of lignite bioorganic fertilizer at 3.0–4.5 t ha^{-1} is appropriate for climate change mitigation in saline-sodic farmlands in the upper Yellow River basin, Northwest China.

CRediT authorship contribution statement

Zhijun Chen: Investigation, Formal analysis, Writing – original draft. **Guanhua Huang:** Supervision, Writing – review & editing. **Yue Li:** Data curation. **Xuechen Zhang:** Investigation. **Yunwu Xiong:** Methodology. **Quanzhong Huang:** Conceptualization. **Song Jin:** Resources.

Declaration of competing interest

The authors declare that they have no known competing financial interests or personal relationships that could have appeared to influence the work reported in this paper.

Acknowledgement

This research was partially supported by the National Natural Science Foundation of China (51639009) and the Key Research Project of Science and Technology in Inner Mongolia Autonomous Region of China (with Numbers 2020, 2021). The authors are grateful to Apaxfon Bioscience and Technology Ltd., Co. for providing their lignite-based fertilizer product (Ginate) and sharing technical and economic data related to the product.

References

Abagandura, G.O., Chintala, R., Sandhu, S.S., Kumar, S., Schumacher, T.E., 2019. Effects of biochar and manure applications on soil carbon dioxide, methane, and nitrous oxide fluxes from two different soils. J. Environ. Qual. 6, 1664–1674. https://doi.org/10.2134/jeq2018.10.0374.

Agegnehu, G., Bass, A.M., Nelson, P.N., Bird, M.I., 2016. Benefits of biochar, compost and biochar–compost for soil quality, maize yield and greenhouse gas emissions in a tropical agricultural soil. Sci. Total Environ. 543, 295–306. https://doi.org/10.1016/j.scitotenv.2015.11.054.

Akimbekov, N., Qiao, X., Digel, I., Abdieva, G., Ualieva, P., Zhubanova, A., 2020. The effect of leonardite-derived amendments on soil microbiome structure and potato yield. Agriculture 10. https://doi.org/10.3390/agriculture10050147.

Bates, S.T., Berg-Lyons, D., Caporaso, J.G., Walters, W.A., Knight, R., Fierer, N., 2011. Examining the global distribution of dominant archaeal populations in soil. ISME J. 5, 908–917. https://doi.org/10.1038/ismej.2010.171.

Bao, S.D., 2000. Soil Agrochemical Analysis. China Agricultural Press, Beijing, China.

Chapman, H.D., 1965. Cation exchange capacity. Methods Soil Analys.: Part 2 Chem. Microbiol. Propert. 9, 891–901.

Daliakopoulos, I.N., Tsanis, I.K., Koutroulis, A., Kourgialas, N.N., Varouchakis, A.E., Karatzas, G.P., Ritsema, C.J., 2016. The threat of soil salinity: a European scale review. Sci. Total Environ. 573, 727–739. https://doi.org/10.1016/j.scitotenv.2016.08.177.

Douglas, G.M., Maffei, V.J., Zaneveld, J., Yurgel, S.N., Brown, J.R., Taylor, C.M., Huttenhower, C., Langille, M.G., 2019. PICRUSt2: an improved and extensible approach for metagenome inference. bioRxiv, 672295. https://doi.org/10.1101/672295.

Dubey, A.N., Raha, P., Kundu, A., 2019. Response of soil applied lignite coal derived humic acid on yield and quality of spinach (Spinacia oleracea L.). Vegetable Sci. 46, 72–77.

Ghosh, U., Thapa, R., Desutter, T., Yangbo, H.E., Chatterjee, A., 2017. Saline-sodic soils: potential sources of nitrous oxide and carbon dioxide emissions? Pedosphere 27 (1), 65–75. https://doi.org/10.3923/ja.2007.480.483.

Guenet, B., Gabrielle, B., Chenu, C., Arrouays, D., Balesdent, J., Bernoux, M., Zhou, F., 2021. Can N_2O emissions offset the benefits from soil organic carbon storage? Global Change Biol. 27 (2), 237–256. https://doi.org/10.1111/gcb.15342.

Hayakawa, A., Akiyama, H., Sudo, S., Yagi, K., 2009. N_2O and NO emissions from an Andisol field as influenced by pelleted poultry manure. Soil Biol. Biochem. 41, 521–529. https://doi.org/10.1016/j.soilbio.2008.12.011.

IPCC, 2021. Summary for Policymakers. In: Climate Change 2021: the Physical Science Basis. Contribution of Working Group I to the Sixth Assessment Report of the Intergovernmental Panel on Climate Change. Cambridge University Press (in press).

Kelly, C.N., Schwaner, G.W., Cumming, J.R., Driscoll, T.P., 2021. Metagenomic reconstruction of nitrogen and carbon cycling pathways in forest soil: influence of different hardwood tree species. Soil Biol. Biochem. 156, 108226 https://doi.org/10.1016/j.soilbio.2021.108226.

Li, C., Xiong, Y., Huang, Q., Xu, X., Huang, G., 2020. Impact of irrigation and fertilization regimes on greenhouse gas emissions from soil of mulching cultivated maize (Zea mays L.) field in the upper reaches of Yellow River, China. J. Clean. Prod. 259, 120873 https://doi.org/10.1016/j.jclepro.2020.120873.

Li, C., Xiong, Y., Zou, J., Dong, L., Ren, P., Huang, G., 2021. Impact of biochar and lignite-based amendments on microbial communities and greenhouse gas emissions from agricultural soil. Vadose Zone J. 20, e20105 https://doi.org/10.1002/vzj2.20105.

Little, K.R., Rose, M.T., Jackson, W.R., Cavagnaro, T.R., Patti, A.F., 2014. Do lignite-derived organic amendments improve early-stage pasture growth and key soil biological and physicochemical properties? Crop Pasture Sci. 65 (9), 899–910. https://doi.org/10.1071/CP13433.

Liu, C., Yao, Z., Wang, K., Zheng, X., Li, B., 2019. Net ecosystem carbon and greenhouse gas budgets in fiber and cereal cropping systems. Sci. Total Environ. 647, 895–904. https://doi.org/10.1016/j.scitotenv.2018.08.048.

Loper, S., Shober, A.L., Wiese, C., Denny, G.C., Stanley, C.D., Gilman, E.F., 2010. Organic soil amendment and tillage affect soil quality and plant performance in simulated residential landscapes. Hortscience 45 (10), 1522–1528. https://doi.org/10.1590/S0102-05362010000400020.

Lozupone, C.A., Knight, R., 2007. Global patterns in bacterial diversity. Proc. Natl. Acad. Sci. U. S. A 104, 11436–11440. https://doi.org/10.1073/pnas.0611525104.

Magoč, T., Salzberg, S.L., 2011. FLASH: fast length adjustment of short reads to improve genome assemblies. Bioinformatics 27 (21), 2957–2963. https://doi.org/10.1093/bioinformatics/btr507.

Mahmood, F., Khan, I., Ashraf, U., Shahzad, T., Hussain, S., Shahid, M., Ullah, S., 2017. Effects of organic and inorganic manures on maize and their residual impact on soil physico-chemical properties. J. Soil Sci. Plant Nutr. 17 (1), 22–32. https://doi.org/10.4067/S0718-95162017005000002.

Nan, J., Chen, X., Chen, C., Lashari, M.S., Du, Z., 2015. Impact of flue gas desulfurization gypsum and lignite humic acid application on soil organic matter and physical properties of a saline-sodic farmland soil in eastern China. J. Soils Sediments 16 (9), 1–11. https://doi.org/10.1007/s11368-016-1419-0.

Pathak, H., 2015. Review: common attributes of hydraulically fractured oil and gas production and CO_2 geological sequestration. Greenh. Gases Sci. Technol. 2, 352–368. https://doi.org/10.1002/ghg.1300.

Paustian, K., Lehmann, J., Ogle, S., Reay, D., Robertson, G.P., Smith, P., 2016. Climate-smart soils. Nature 532, 49–57. https://doi.org/10.1038/nature17174.

Praeg, N., Wagner, A.O., Illmer, P., 2016. Plant species, temperature, and bedrock affect net methane flux out of grassland and forest soils. Plant Soil 1–14. https://doi.org/10.1007/s11104-016-2993-z.

Qi, L., Pokharel, P., Chang, S.X., Zhou, P., Niu, H., He, X., Wang, , et al.Gao, M., 2020. Biochar application increased methane emission, soil carbon storage and net ecosystem carbon budget in a 2-year vegetable–rice rotation. Agric. Ecosyst. Environ. 292, 106831 https://doi.org/10.1016/j.agee.2020.106831.

Rath, K.M., Fierer, N., Murphy, D.V., Rousk, J., 2018. Linking bacterial community compo- sition to soil salinity along environmental gradients. ISME J. 13, 836–846. https://doi.org/10.1038/s41396-018-0313-8.

Ray, R.L., Griffin, R.W., Fares, A., Elhassan, A., Awal, R., Woldesenbet, S., Risch, E., 2020. Soil CO_2 emission in response to organic amendments, temperature, and rainfall. Sci. Rep. 10, 1–14. https://doi.org/10.1038/s41598-020-62267-6.

Schwaner, G.W., Kelly, C.N., 2019. American chestnut soil carbon and nitrogen dynamics: implications for ecosystem response following restoration. Pedobiologia 75, 24–33. https://doi.org/10.1016/j.pedobi.2019.05.003.

Shakoor, A., Shahzad, S.M., Chatterjee, N., Arif, M.S., Farooq, T.H., Altaf, M.M., Tufail, M.A., Dar, A.A., Mehmood, T., 2021b. Nitrous oxide emission from agricultural soils: application of animal manure or biochar? A global meta-analysis. J. Environ. Manag. 285, 112170 https://doi.org/10.1016/j.jenvman.2021.112170.

Shakoor, A., Shahzad, S.M., Farooq, T.H., Ashraf, F., 2020. Future of ammonium nitrate after Beirut (Lebanon) explosion. Environ. Pollut. 267, 115615 https://doi.org/10.1016/j.envpol.2020.115615.

Shakoor, A., Shakoor, S., Rehman, A., Ashraf, F., Abdullah, M., Shahzad, S.M., Farooq, T. H., Ashraf, M., Manzoor, M.A., Altaf, M.A., 2021a. Effect of animal manure, crop type, climate zone, and soil attributes on greenhouse gas emissions from agricultural soils—a global meta-analysis. J. Clean. Prod. 124019 https://doi.org/10.1016/j.jclepro.2020.124019.

Tang, J., Liang, S., Li, Z., Zhang, H., Wang, S., Zhang, N., 2016. Emission laws and influence factors. of greenhouse gases in saline-alkali paddy fields. Sustainability 8 (2), 163. https://doi.org/10.3390/su8020163.

Thangarajan, R., Bolan, N.S., Tian, G., Naidu, R., Kunhikrishnan, A., 2013. Role of organic amendment application on greenhouse gas emission from soil. Sci. Total Environ. 465, 72–96. https://doi.org/10.1016/j.scitotenv.2013.01.031.

Tran, C.K.T., Rose, M.T., Cavagnaro, T.R., Patti, A.F., 2015. Lignite amendment has limited impacts on soil microbial communities and mineral nitrogen availability. Appl. Soil Ecol. 95, 140–150. https://doi.org/10.1016/j.apsoil.2015.06.020.

Tsetsegmaa, G., Akhmadi, K., Cho, W., Lee, S., Chandra, R., Jeong, C.E., Kang, H., 2018. Effects of oxidized brown coal humic acid fertilizer on the relative height growth rate of three tree species. Forests 9 (6), 360. https://doi.org/10.3390/f9060360.

Wang, C., Shen, J., Zheng, L., Liu, Y., Qin, H., Wu, J., 2014. Effects of combined applications of pig manure and chemical fertilizers on CH_4 and N_2O emissions and their global warming potentials in paddy fields with double-rice cropping. Environ. Sci. 35, 3121–3127.

Wang, C., Shen, J.L., Liu, J.Y., Qin, H.L., Yuan, Q., Fan, F.L., Hu, Y.J., Wang, J., Wei, W. X., Li, Y., Wu, J.S., 2019. Microbial mechanisms in the reduction of CH_4 emission from double rice cropping system amended by biochar: a four-year study. Soil Biol. Biochem. 135, 251–263. https://doi.org/10.1016/j.soilbio.2019.05.012.

Wu, L., Wu, X., Lin, S., Wu, Y., Tang, S., Zhou, M., Ahaaban, M., Zhao, J., Hu, R., Kuzyakov, Y., Wu, J., 2018. Carbon budget and greenhouse gas balance during the initial years after rice paddy conversion to vegetable cultivation. Sci. Total Environ. 627, 46–56. https://doi.org/10.1016/j.scitotenv.2018.01.207.

Yang, C., Lv, D., Jiang, S., Lin, H., Sun, J., Li, K., Sun, J., 2021. Soil salinity regulation of soil. microbial carbon metabolic function in the Yellow River Delta, China. Sci. Total Environ. 790, 148258 https://doi.org/10.1016/j.scitotenv.2021.148258.

Yang, W., Feng, G., Miles, D., Gao, L., Jia, Y., Li, C., Qu, Z., 2020. Impact of biochar on greenhouse gas emissions and soil carbon sequestration in corn grown under drip irrigation with mulching. Sci. Total Environ. 729, 138752 https://doi.org/10.1016/j.scitotenv.2020.138752.

Zaman, M., Shahid, S.A., Heng, L., 2018. Guideline for Salinity Assessment, Mitigation and Adaptation Using Nuclear and Related Techniques.

Zhang, H., Tang, J., Liang, S., Li, Z., Yang, P., Wang, J., Wang, S., 2017. The emissions of carbon. dioxide, methane, and nitrous oxide during winter without cultivation in local saline-alkali rice and maize fields in Northeast China. Sustainability 9 (10), 1916. https://doi.org/10.3390/su9101916.

Zhang, Q., Zhou, W., Liang, G., Wang, X., Sun, J., He, P., Li, L., 2015. Effects of different organic manures on the biochemical and microbial characteristics of albic paddy soil in a short-term experiment. PLoS One 10 (4), 0124096. https://doi.org/10.1371/journal.pone.0124096.

Zhang, T., Liu, H., Luo, J., Wang, H., Zhai, L., Geng, Y., Zhang, Y., Li, J., Lei, Q., Bashir, M.A., Wu, S., Lindsey, S., 2018. Long-term manure application increased greenhouse gas emissions but had no effect on ammonia volatilization in a Northern China upland field. Sci. Total Environ. 633, 230–239. https://doi.org/10.1016/j.scitotenv.2018.03.069.

Zhao, Q., Bai, J., Gao, Y., Zhao, H., Zhang, G., Cui, B., 2020. Shifts in the soil bacterial com- munity along a salinity gradient in the Yellow River Delta. Land Degrad. Dev. 31, 2255–2267. https://doi.org/10.1038/srep36550.

Zhen, Z., Liu, H., Wang, N., Guo, L., Meng, J., Ding, N., Jiang, G., 2014. Effects of manure compost application on soil microbial community diversity and soil microenvironments in a temperate cropland in China. PLoS One 9 (10), 108555. https://doi.org/10.1371/journal.pone.0108555.

Zhou, M., Butterbach-Bahl, K., Vereecken, H., Brüggemann, N., 2017. A meta-analysis of soil. salinization effects on nitrogen pools, cycles and fluxes in coastal ecosystems. Global Change Biol. 23, 1338–1352. https://doi.org/10.1111/gcb.13430.